Drozdov, A. Y., Shprits, Y., Aseev, N., Kellerman, A. C., Reeves, G. D. (2017): Dependence of radiation belt simulations to assumed radial diffusion rates tested for two empirical models of radial transport. - *Space Weather*, *15*, 1, pp. 150—162.

DOI: http://doi.org/10.1002/2016SW001426

AGU PUBLICATIONS

Space Weather

RESEARCH ARTICLE
10.1002/2016SW001426

Key Points:
- The difference between simulations with either of the considered radial diffusion parameterizations is negligible
- 3-D simulations are less sensitive to the assumed parameterization of the radial diffusion rates than 1-D simulations
- Multiplication of the radial diffusion rates by a constant factor leads to unrealistic results

Supporting Information:
- Supporting Information S1

Correspondence to:
A. Y. Drozdov,
adrozdov@ucla.edu

Citation:
Drozdov, A. Y., Y. Y. Shprits, N. A. Aseev, A. C. Kellerman, and G. D. Reeves (2017), Dependence of radiation belt simulations to assumed radial diffusion rates tested for two empirical models of radial transport, *Space Weather*, *15*, 150–162, doi:10.1002/2016SW001426.

Received 12 MAY 2016
Accepted 27 DEC 2016
Accepted article online 30 DEC 2016
Published online 20 JAN 2017

Dependence of radiation belt simulations to assumed radial diffusion rates tested for two empirical models of radial transport

A. Y. Drozdov[1], Y. Y. Shprits[1,2,3], N. A. Aseev[1,2,3], A. C. Kellerman[1], and G. D. Reeves[4]

[1]Department of Earth, Planetary, and Space Sciences, University of California, Los Angeles, California, USA, [2]GFZ German Research Centre For Geosciences, Potsdam, Germany, [3]Institute of Physics and Astronomy, University of Potsdam, Potsdam, Germany, [4]Space Science and Applications Group, Los Alamos National Laboratory, Los Alamos, New Mexico, USA

Abstract Radial diffusion is one of the dominant physical mechanisms that drives acceleration and loss of the radiation belt electrons, which makes it very important for nowcasting and forecasting space weather models. We investigate the sensitivity of the two parameterizations of the radial diffusion of Brautigam and Albert (2000) and Ozeke et al. (2014) on long-term radiation belt modeling using the Versatile Electron Radiation Belt (VERB). Following Brautigam and Albert (2000) and Ozeke et al. (2014), we first perform 1-D radial diffusion simulations. Comparison of the simulation results with observations shows that the difference between simulations with either radial diffusion parameterization is small. To take into account effects of local acceleration and loss, we perform 3-D simulations, including pitch angle, energy, and mixed diffusion. We found that the results of 3-D simulations are even less sensitive to the choice of parameterization of radial diffusion rates than the results of 1-D simulations at various energies (from 0.59 to 1.80 MeV). This result demonstrates that the inclusion of local acceleration and pitch angle diffusion can provide a negative feedback effect, such that the result is largely indistinguishable simulations conducted with different radial diffusion parameterizations. We also perform a number of sensitivity tests by multiplying radial diffusion rates by constant factors and show that such an approach leads to unrealistic predictions of radiation belt dynamics.

1. Introduction

Captured by the Earth's magnetic field, energetic electrons and protons form the radiation belts. The outer electron belt is highly dynamic and has been observed and studied since the beginning of the space age [*Van Allen and Frank*, 1959]. However, prediction and understanding of the energetic electron population variation remain a challenging task [*Reeves et al.*, 2003; *Shprits et al.*, 2008a, 2008b]. Since energetic electrons create a hazardous environment for Earth-orbiting satellites and the international space station, the understanding and prediction of the radiation belts dynamics are very important. Radiation belt models [e.g., *Li*, 2004; *Subbotin and Shprits*, 2009; *Reeves et al.*, 2012; *Su et al.*, 2010; *Varotsou et al.*, 2008; *Albert et al.*, 2009] simulate radial transport by using various radial diffusion parameterizations. As results of the simulations may depend on these parameterizations, it is important for space weather modeling and prediction to investigate how the choice of the radial diffusion models may affect simulation results. In the study we analyze the response of radiation belt modeling to commonly used statistical radial diffusion rates: *Brautigam and Albert* [2000] and *Ozeke et al.* [2014], hereafter denoted as BA and OZ, respectively. As radial diffusion shows significant variability and is driven by the solar wind activity, in this study we have not considered radial diffusion parameterizations that are independent of geomagnetic activity. The detailed comparison between considered different radial diffusion parameterizations can be useful for the development of current and future space weather models.

Radial diffusion occurs as a result of the violation of the third adiabatic invariant of motion due to the resonant interactions between ultralow-frequency (ULF) waves and electrons [*Kellogg*, 1959; *Fälthammar*, 1965; *Roederer*, 1970]. Depending on the phase space density (PSD) gradient, radial diffusion moves electrons inward or outward from the Earth, which accelerates or decelerates the electrons, respectively. By working as a loss or a source of high-energy electrons, radial diffusion transport plays an important role in the formation and structure of the outer electron radiation belt and is important for electron acceleration [e.g., *Shprits and Thorne*, 2004; *Su et al.*, 2015] and loss [e.g., *Reeves et al.*, 1998; *Desorgher et al.*, 2000; *Miyoshi et al.*, 2003; *Shprits et al.*, 2005]. *Shprits et al.* [2006] showed that outward radial diffusion may also provide a very effective loss down to L ~ 4 during the main phase of a storm, when loss to the magnetopause results in negative gradients in PSD. They also showed that the outward radial diffusion can often explain observed dropouts in PSD during a storm's main phase. This explanation for a dropout has been confirmed by observations from NOAA Polar-orbiting Operational Environmental Satellites that measure precipitating particles [*Turner et al.*, 2012]. *Su et al.* [2015] discussed that radial diffusion can play a dominant role of the radiation belt electron acceleration for specific events. Although the electron acceleration due to the local process is more common, radial diffusion redistributes the electrons along the radial direction smoothing PSD gradients, which makes it an important part of radiation belt dynamics.

ULF waves can be separated into electrostatic and electromagnetic wave components [*Schulz and Lanzerotti*, 1974] with corresponding electrostatic (D_{LL}^{ES}) and electromagnetic (D_{LL}^{EM}) diffusion coefficients. The total radial diffusion coefficient includes both components and was studied previously [e.g., *Fälthammar*, 1965; *Brautigam and Albert*, 2000]:

$$D_{LL} = D_{LL}^{ES} + D_{LL}^{EM}. \tag{1}$$

Radial diffusion occurs due to the resonance of the electron drift motion with an electromagnetic field perturbation. The resonance condition for the drift resonance may be written as

$$\Omega_{\mathrm{ULF}} = m\Omega_D, \tag{2}$$

where Ω_{ULF} is the Fourier harmonic of the wave frequency, m is the number of the harmonic, and Ω_D is the drift frequency.

To calculate the diffusion coefficient, the ULF wave amplitude characteristic needs to be known. The fluctuation of magnetic and electric fields can be described by the power spectral density of the corresponding components of the ULF waves. Summing over all the resonances, the diffusion coefficient can be expressed as [*Schulz and Lanzerotti*, 1974; e.g., *Fei et al.*, 2006; *Ozeke et al.*, 2012]:

$$D_{LL}^{E} \propto L^6 \sum_m P_E{}^m (m\Omega_D), \tag{3}$$

$$D_{LL}^{M} \propto L^8 \Omega_D{}^2 \sum_m m^2 P_M{}^m (m\Omega_D), \tag{4}$$

where $P_{E,M}{}^m$ is the power spectral density of electric and magnetic components that respectively depends on the drift frequency and the harmonic number in equation (2); L is McIlwain L shell.

There are various approaches that provide radial diffusion coefficients. *Fei et al.* [2006] proposed the event-based method of the radial diffusion coefficients calculation. Using the ULF electric and magnetic field power spectral density obtained from the global magnetohydrodynamics (MHD) simulation of the specific events (September 1998 storm), the authors constructed the time-dependent radial diffusion rates that were used in the 1-D Fokker-Plank equation simulation to describe the dynamics of the PSD evolution. This approach requires a computationally expensive MHD modeling for the considered period of time, and it can be difficult to apply in long-term simulations or real-time prediction models. *Su et al.* [2015] used a data-driven method of the radial diffusion rate calculation. The power spectral density was obtained directly from the measurements and used in the radial diffusion calculations. Following this approach in combination with the 1-D radial diffusion simulation, the authors were able to reproduce the acceleration of the electrons due to the radial transport for specific events. Another model was proposed by *Fok et al.*, 2008, these authors did not account for the radial diffusion term explicitly, but the model included a time-varying magnetic field.

Validation of the storm-specific models is a challenging task, as the relative success of the models may turn out to be a simple coincidence. Another challenge comes from the fact that there are currently no standardized procedures for code validation, and models are compared by different measures. The statistical and empirical models of radial diffusion coefficients provide the parameterization for long-term simulations that can be validated in a statistical and systematic way. Such models can be used in the future for space weather modeling.

The radial diffusion model proposed by *Brautigam and Albert* [2000] is based on the empirically determined value of the electromagnetic diffusion coefficient D_{LL}^{EM} parameterized by *Kp* index:

$$D_{LL}^{EM} = L^{10} 10^{(0.506\ Kp\ -\ 9.325)}\ [1/\mathrm{day}],\ Kp = 1\ \text{to}\ \ 6, \tag{5}$$

and electrostatic diffusion coefficient DLL_{ES} calculated from the electric field amplitudes parameterized as a linear function of Kp index:

$$D_{LL}^{\mathrm{ES}} = L^6 \, \frac{1}{4} \left(\frac{10^3(0.26(Kp-1)+0.1)}{0.311} \right)^2 \left(\frac{2700}{1+(1350 \ \Omega_D)^2} \right) \left[\mathrm{cm}^2/s \right], \ Kp = 1 \ \text{ to } 6, \tag{6}$$

where exponential decay time for the electric-field impulse is determine as 2700 s (0.75 h) and Ω_D is determined in hertz.

In their paper, the authors analyzed the response of outer radiation belt electrons to the 9 October 1990 magnetic storm. This analysis included the simulation of radial diffusion transport and comparison of the results with observations from Combined Release and Radiation Effects Satellite (CRRES) [*Vampola et al.*, 1992].

The simulation was based on solving the modified Fokker-Planck equation [*Walt*, 1970] which describes radial diffusion with parameterized losses:

$$\frac{\partial f}{\partial t} = L^2 \frac{\partial}{\partial L} \left[\frac{1}{L^2} \langle D_{LL} \rangle \frac{\partial f}{\partial L} \right] - \frac{f}{\tau_{\mathrm{param}}} , \tag{7}$$

where f is electron phase space density defined as a function of adiabatic invariants (μ, J, and L) and τ_{param} is the time scale of losses, μ is the first adiabatic invariant, and J is the second adiabatic invariant. The diffusion coefficient D_{LL} is a summation of D_{LL}^{ES} (equation (6)) and D_{LL}^{EM} (equation (5)) diffusion coefficients corresponding to the electrostatic and electromagnetic wave-particle interaction respectively; both coefficients are parameterized with Kp index. The electrostatic coefficient D_{LL}^{ES} from *Cornwall* [1968] was computed by using the root-mean-square of the electric field amplitude assumed to be a linear function of the Kp index. This parameterization is consistent with rates used in previous studies for geomagnetic quiet time [*Lyons and Thorne*, 1973] and active time [*Lyons and Schulz*, 1989]. To obtain the Kp-dependent D_{LL}^{EM} diffusion coefficient, authors used empirically obtained diffusion coefficients for different L. At $L = 4$, the electromagnetic coefficient was based on ground measurements [*Lanzerotti and Morgan*, 1973], and for $L = 6.6$, this coefficient was calculated based on geosynchronous measurements [*Lanzerotti and Webb*, 1978].

Kim et al. [2011] showed that the Versatile Electron Radiation Belt (VERB) code [*Subbotin and Shprits*, 2009; *Subbotin et al.*, 2010] simulation that includes the *Brautigam and Albert* [2000] electrostatic diffusion coefficient D_{LL}^{ES} (equation (6)) overestimated fluxes in the slot region and in the inner belt. It was concluded that the electrostatic coefficient D_{LL}^{ES} needs to be determined more accurately for $L < 3$. In this study we do not include an electrostatic component.

In *Ozeke et al.* [2014] the total radial diffusion coefficient was separated into two terms due to the azimuthal electric field:

$$D_{LL}^{E} = L^6 \ 2.6 \cdot 10^{-8} 10^{(0.217L + 0.461Kp)}, \ [1/\mathrm{day}], \tag{8}$$

and the compressional magnetic field of the ULF waves:

$$D_{LL}^{M} = L^8 \ 6.62 \cdot 10^{-13} 10^{\left(-0.0327L^2 + 0.625L - 0.0108Kp^2 + 0.499Kp\right)}, \ [1/\mathrm{day}]. \tag{9}$$

The electric diffusion coefficient D_{LL}^{E} was determined from 15 years of ground measurements. In situ determination required a series of simultaneous measurements in space. Since this approach is almost always impossible, the authors were using the ground-based magnetometer measurements and an Alfvénic wave mapping model in a dipole field following [*Ozeke et al.*, 2009; *Rae et al.*, 2012] to determine the azimuthal component of the equatorial electric field and estimate power spectral density ${P_E}^m$ in equation (3). *Ozeke et al.* [2014] used frequency-independent electric field power spectral density. As a result, D_{LL}^{E} in equation (8) does not depend on the electron's μ value. Additionally, only guided Alfvén waves were used to avoid twice counting the azimuthal component of the compressional wave. The calculation of the magnetic diffusion coefficient D_{LL}^{M} in equation (5) was also based on in situ measurements. The component ${P_M}^m$ in equation (4) was obtained by the GOES and the Active Magnetospheric Particle Tracer Explorers spacecraft measurements [*Ozeke et al.*, 2012] in the period from 1996 to 2005. It should be noted that the electromagnetic field diffusion coefficients of the *Brautigam and Albert* [2000] model are not based on in situ measurements of power spectral density. Thus, using the new model that is based on in situ observations may provide more accurate results in the radiation belt simulation.

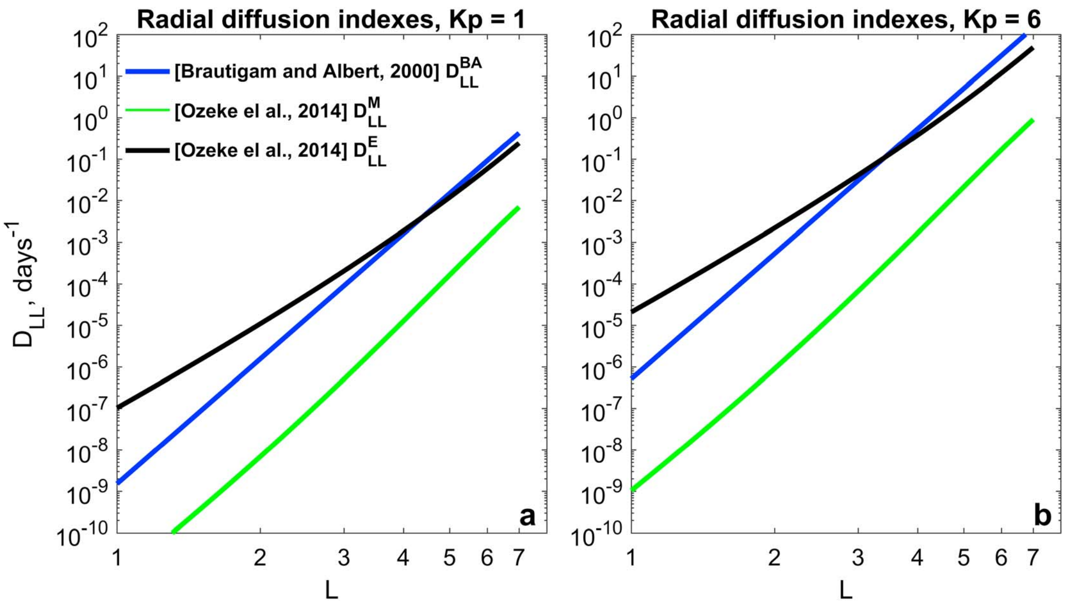

Figure 1. Comparison of radial diffusion coefficients presented in *Brautigam and Albert* [2000] (blue indicates electromagnetic component; equation (5)) and presented in *Ozeke et al.* [2014] (green indicates magnetic component; equation (5); black indicates electric component; equation (8)). Total diffusion coefficient (D_{LL}^{O}) from *Ozeke et al.* [2014] is not shown, because it is practically identical to electric component (D_{LL}^{E}) due to negligible magnetic component (D_{LL}^{M}). (a) $Kp = 1$. (b) $Kp = 6$.

Figure 1 shows the comparison of the radial diffusion coefficients related to electromagnetic field fluctuations calculated by *Brautigam and Albert* [2000] ($D_{LL}^{EM} \equiv D_{LL}^{BA}$; equation (5)) with radial diffusion coefficients obtained in *Ozeke et al.* [2014] (azimuthal electric field diffusion coefficient D_{LL}^{E}; equation (8)), compressional magnetic field diffusion coefficients D_{LL}^{M} (equation (5), and total diffusion coefficient $D_{LL}^{O} = D_{LL}^{M} + D_{LL}^{E}$). It can be seen that the electric component D_{LL}^{E} (equation (8)) is dominant over the magnetic component D_{LL}^{M} (equation (5) and the total diffusion coefficient D_{LL}^{O} is defined by the electric component. Comparison of two models shows that the diffusion coefficient D_{LL}^{O} is smaller than D_{LL}^{BA} for $L \gtrsim 4$ and is larger at smaller L shells. Note that the difference between coefficients is less than an order of magnitude at the outer belt region ($L \gtrsim 3$). To quantify the influence of each radial diffusion model to the radiation belt dynamics, it is necessary to perform the diffusion simulation including radial diffusion rates.

In several studies, the authors multiplied radial diffusion rates by a constant factor in order to find a way to improve the 1-D simulation results [e.g., *Tu et al.*, 2009; *Ozeke et al.*, 2014; *Mann et al.*, 2016]. For example, *Ozeke et al.* [2014] showed that the power spectral density of ULF waves can vary from its mean value and suggested that the variation of their diffusion rates may be changed by a factor of 3. A similar approach was used in 3-D simulations as well [e.g., *Tu et al.*, 2013]. The recent study of *Murphy et al.* [2016] suggested that for individual geomagnetic storms, the actual diffusion rates could be 4 orders of magnitude smaller or larger than those predicted by an empirical model derived as a function of *Kp*. Such diffusion rates are very difficult to validate. For instance, in an individual storm, the relative success of a radiation belt model at a particular energy may result from a balance of several inaccurate parameterizations and potentially missing physical processes.

In this study, we investigate the sensitivity of the long-term VERB code simulations to the assumed parameterization of radiation diffusion. We compare results between different simulations and with observations. Following *Brautigam and Albert* [2000] and *Ozeke et al.* [2014], we first perform 1-D radial diffusion simulations with realistic upper boundary condition and parameterized losses. To take into account local acceleration and loss due to wave-particle interactions, we then perform a 3-D simulation and compare it with results of 1-D simulations. The comparison of 3-D simulations with 1-D simulations reveals the contribution of the local diffusion processes to the radiation belt dynamics. To investigate how sensitive the model results are to the choice of the parameterizations, we compare the simulations with observations. Finally, we perform a number of sensitivity tests using the VERB code to investigate the reliability of the approach of multiplying the radial diffusion rate by a constant factor.

2. Modeling and Observational Comparison

2.1. VERB Code

The Versatile Electron Radiation Belt code is a powerful tool for performing diffusion simulations. The VERB code can be easily used for 1-D simulations similar to the simulations described by *Brautigam and Albert* [2000] or *Ozeke et al.* [2014]. In addition, more comprehensive 3-D simulations can be performed by using the VERB code.

The 1-D Fokker-Planck equation (7) includes only the radial diffusion process due to the violation of the third adiabatic invariant. The violation of the first and the second invariants can be written as the bounce-averaged diffusion equation in terms of equatorial pitch angle and energy following *Schulz and Lanzerotti* [1974]. Thus, to take into account both described processes, the modified Fokker-Planck equation may be rewritten [*Shprits et al.*, 2008b] and solved on two different computational grids that preserve the first and second invariants during radial transport and another that preserves orthogonality in momentum and pitch angle. We use the formulation of the Fokker Planck equation in terms of invariants (*L*, *V*, and *K*) to avoid interpolation between two grids [*Subbotin and Shprits*, 2012]:

$$\begin{aligned}\frac{\partial f}{\partial t} = &\frac{1}{G}\frac{\partial}{\partial L}\bigg|_{V,K}\left[G\langle D_{LL}\rangle\frac{\partial f}{\partial L}\bigg|_{V,K}\right] + \frac{1}{G}\frac{\partial}{\partial V}\bigg|_{L,K}\left[G\left(\langle D_{VV}\rangle\frac{\partial f}{\partial V}\bigg|_{L,K} + \langle D_{VK}\rangle\frac{\partial f}{\partial K}\bigg|_{L,V}\right)\right] \\ &+ \frac{1}{G}\frac{\partial}{\partial K}\bigg|_{L,V}\left[G\left(\langle D_{KK}\rangle\frac{\partial f}{\partial K}\bigg|_{L,V} + \langle D_{VK}\rangle\frac{\partial f}{\partial V}\bigg|_{L,K}\right)\right] - \frac{f}{\tau},\end{aligned} \tag{10}$$

where K and V are adiabatic invariants; $K = J/\sqrt{8\ \mu m_0}$, where m_0 is electron rest mass; $V \equiv \mu \cdot (K+0.5)^2$; $\langle D_{KK}\rangle, \langle D_{VV}\rangle, \langle D_{VK}\rangle$ are diagonal and mixed diffusion coefficients; $G = -2\pi B_0 R_E^2 L^{-2}\sqrt{8\ \mu m_0}/(K+0.5)^2$ is the Jacobian of the transformation from an adiabatic invariant system (μ, J, and Φ), where Φ is third adiabatic invariant to the (V, K, and L) coordinate system; R_E is the Earth's radius, $B_0 = 0.3$; G is the field on the equator at the Earth's surface; and f/τ represents losses inside the loss cone with τ being equal to a quarter bounce period inside the loss cone and infinitely outside of the loss cone. This approach allows setting up convenient boundary conditions inside the loss cone which is impossible if (μ, J, L) coordinates are used.

Equations (7) and (8) can be solved by the VERB code in 1-D and 3-D simulations, respectively. *Shprits et al.* [2005] used equation (7) to quantify the competing effects on the distribution of the outer zone relativistic electrons of inward radial diffusion described by BA and losses. The model was capable of predicting the radial extent of high-energy fluxes and locations of peak fluxes for many storms and predicts MeV electron fluxes within 1 order of magnitude accuracy for most of the simulation time and most L values. *Subbotin et al.* [2011] performed a long-term simulation solving equation (8) by using BA diffusion rates and showed good agreement between modeling and CRRES observations and between modeling and satellite reanalysis for a long time period, including the 9 October 1990 geomagnetic storm. *Drozdov et al.* [2015] also confirmed that the VERB code is capable of reproducing the dynamics of the energetic and relativistic electrons as the result of the long-term simulation and comparison with the Van Allen Probe [*Mauk et al.*, 2013; *Stratton et al.*, 2014] measurements.

2.2. 1-D Simulations With Realistic Boundary Conditions

There are many factors that affect the modeling of radiation belt dynamics. To show how the considered radial diffusion coefficients affect the solution of the diffusion equations, we first perform 1-D simulations in order to compare with previously published results.

A 1 year period from 1 October 2012 to 1 October 2013 (see Figure 2) was chosen to investigate the influence of the *Kp*-dependent radial diffusion model on the results of the 1-D simulation. The outer boundary conditions were obtained from Van Allen Probes Magnetic Electron Ion Spectrometer (MagEIS) [*Blake et al.*, 2013]. The steady state radial diffusion solution was used as an initial condition. The parameterizations of the losses were the same as in the 1-D simulation performed by *Ozeke et al.* [2014]. We use analytic expressions for the *Kp*-dependent electron lifetime, τ outside the plasmasphere from Shprits *et al.* [2005]; however, the

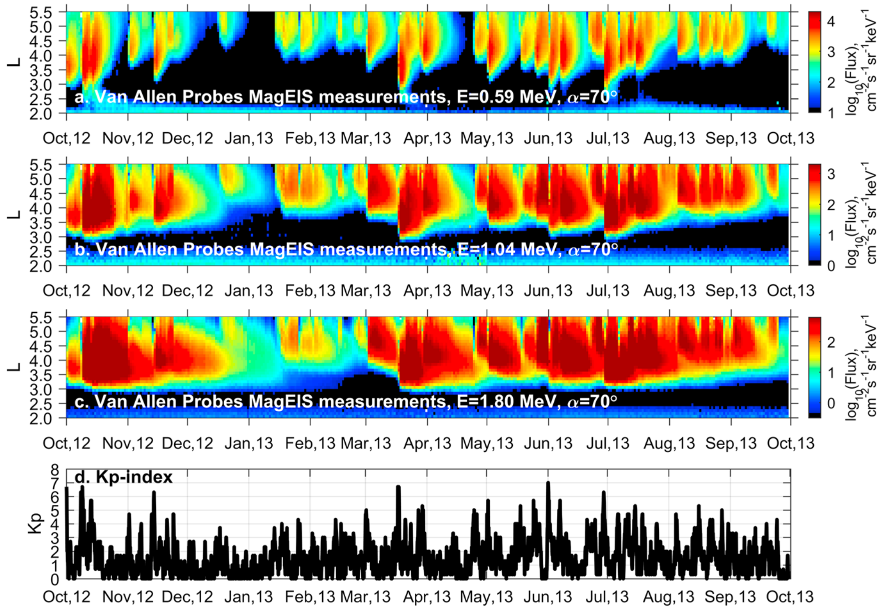

Figure 2. (a–c) Van Allen Probe MagEIS measurements of electron flux at 0.56, 1.04, and 1.80 MeV, respectively, at pitch angle $\alpha = 70°$; (d) *Kp* index.

dependence was multiplied by a factor of 2 ($\tau = 6/Kp$ days) similar to *Ozeke et al.* [2014]. Inside the plasmasphere, the electron lifetime was set to 10 days. The plasmapause location was calculated following *Carpenter and Anderson* [1992].

Ozeke et al. [2014] conducted 1-D simulations and considered only electrons at 0.976 MeV, while in this study we extend the comparison to include a broader range of electron energies. This choice was made because for higher energy, the azimuthal transport is dominated by the gradient-curvature drift, while for lower energies the induced electric field drift is more pronounced. The results of the simulations with different radial diffusion rates, comparison of the simulation results with observations, and comparison between the simulations are shown in Figure 3. To quantify the difference between simulations and between the model and observations, the normalized difference (ND) was constructed by using the following equation [*Subbotin and Shprits*, 2009]:

$$\mathrm{ND}(L,t) = \frac{\mathrm{Flux}_1(L,t) - \mathrm{Flux}_2(L,t)}{\max|_{\text{over } L \text{ at const } t}\ \frac{\mathrm{Flux}_1(L,t)+\mathrm{Flux}_2(L,t)}{2}}, \quad (11)$$

where Flux_1 and Flux_2 are comparable electron fluxes obtained from different simulations or from the measurements and a simulation. This metric shows the difference between the electron fluxes, which is normalized by the average maximum flux for a given time. The chosen metric emphasizes the difference which is significant in comparison with the average value of the flux maximized over L for each time. Eventually, the maximum value of electron flux and its location are more important in considering radiation hazards. It emphasizes how well the simulation can reproduce the flux peaks and flux profiles around the maximum. In case of the comparison between two simulations, it indicates the difference in the heart of the radiation belt and excludes the areas of the low flux values, such as the slot region to avoid comparison of very small numbers.

Figure 3 presents a comparison of the evolution of 0.56 MeV, 1.04 MeV, and 1.80 MeV observed on Van Allen Probes (Figures 3a–3c), obtained from 1-D simulations using BA parameterizations (Figures 3d–3f) and OZ parameterizations (Figures 3g–3i). Comparison between measurements and simulation with the BA parameterization is shown in Figures 3j–3l, and comparison between measurements and simulation with OZ is shown in Figures 3m–3o.

As a reference value that can describe the overall accuracy of the simulation with one number, we choose the mean value of the absolute ND (hereafter, referred to as the *mean absolute value* and denoted as $<|\mathrm{ND}|>$ in

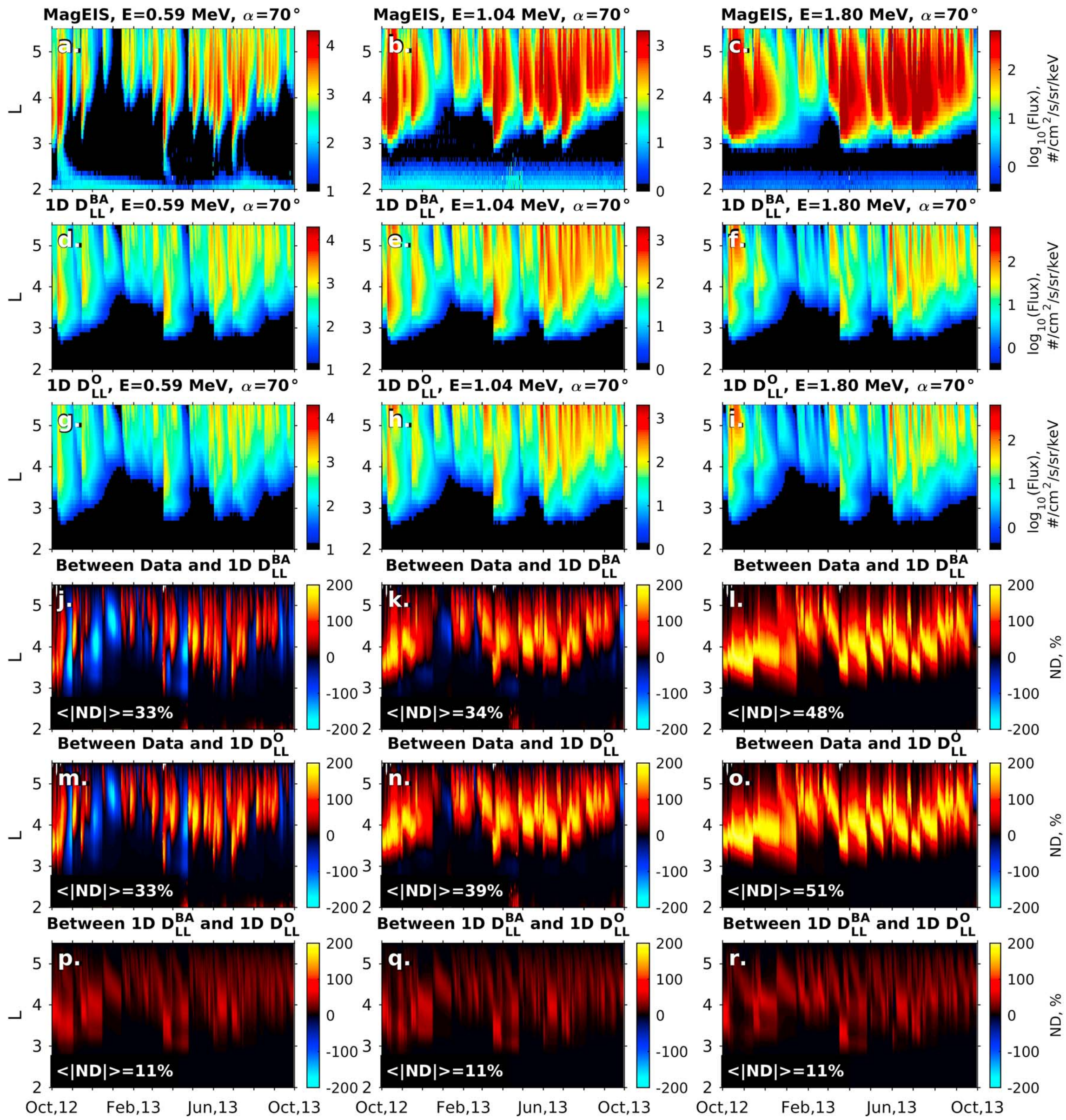

Figure 3. (a–c) Measurements of electron flux at 0.56, 1.04, and 1.80 MeV, respectively, at pitch angle $\alpha = 70°$; (d–f) VERB code simulation with BA and (g–i) with OZ parameterizations; (j–l) normalized difference between simulations with BA parameterization and measurements; (m–o) difference between simulations with OZ parameterization and measurements; and (p–r) normalized difference between simulation with BA and with OZ parameterizations. The mean absolute value is presented on every ND panel.

figures). The distribution of the obtained NDs is positively skewed (Figure S3 in the Supporting Information S1 shows the examples of the distribution histogram). For this kind of distribution, the median better characterizes the expected value; however, in this case we are not interested in the expected value; rather, we are interested in the cumulative difference across all L shells and time. We choose to normalize the sum of all absolute values of NDs by the number of grid cells, which is equal to the mean value. For the mean absolute value calculations, the ND distributions of the whole period of time (1 year) at a fixed energy were spatially limited in the range of L shells from 2.0 to 5.5. The same range is shown in every figure of the NDs. The mean absolute values are presented on each panel of NDs in Figures 3 and 4.

Figures 3d–3i show that both simulations, in general, capture the general dynamics of the radiation belt, covering the period of various geomagnetic activity (see *Kp* index in Figure 2d) However, the simulations do not qualitatively reproduce the flux peaks at high energies (1.80 MeV), and they overestimated the

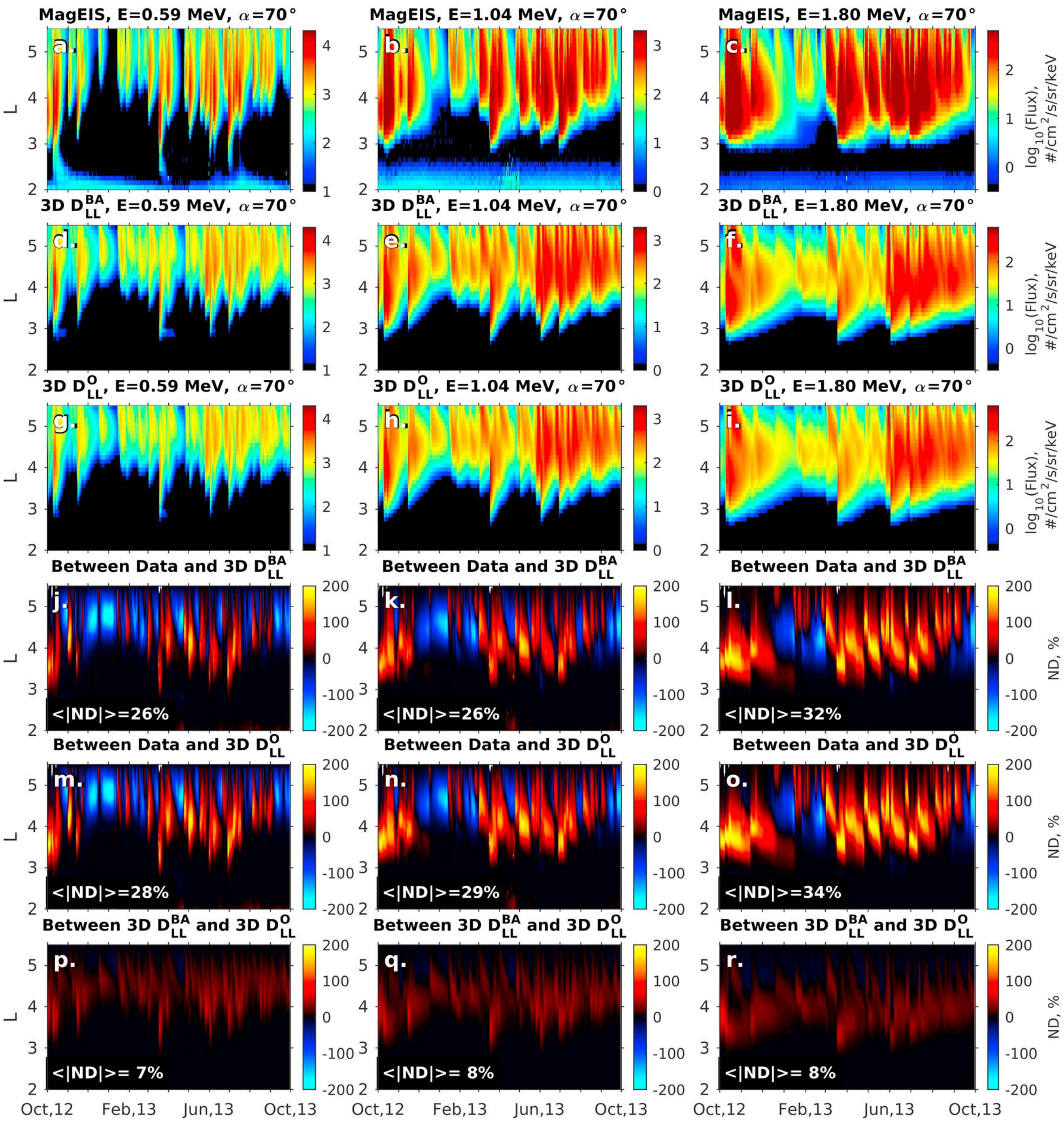

Figure 4. (a–r) Similar to Figure 3 but for 3-D simulations.

measured fluxes at low energies (0.56 MeV). The simulations at 1.04 MeV are closer to the observations than at other energies. The traditional logarithmic difference (LD), which is presented in Figure S1, also confirms these findings. Comparison between simulations with BA and OZ parameterizations (Figures 3p–3r) shows that the presented ND is much lower than the ND between model and observations. The variation of the mean absolute values for the comparison between the model and observations is in the range from 33 to 51%, while the mean absolute values of the comparison between two simulations are lower (around 11%). While there is a difference between the radial diffusion rates for the two parameterizations considered in this study, 1-D simulations differ by a very small factor in comparison to the difference between each of the simulations and observations.

2.3. 3-D Simulations Including Local Diffusion Processes

The 1-D simulations do not fully describe the complexity of the processes that drive radiation belts dynamics, as they rely on a parameterization of the complex loss mechanics caused by local wave-particle interactions.

To improve the model, local diffusion coefficients that correspond to the processes such as pitch angle scattering or energy diffusion must be introduced into a 3-D simulation.

As described in *Shprits et al.* [2008a, 2008b], radial diffusion, local acceleration, and pitch angle diffusion are all coupled to each other, and there are a number of feedback mechanisms between them. For instance, energy diffusion can decrease the radial gradient and slow down inward radial diffusion.

For the 3-D simulation described by equation (8), the outer boundary and initial conditions are the same as in 1-D simulations described in section 2.1. The parameterizations for the pitch angle, momentum, and crossed diffusion coefficients for chorus waves, lightning whistlers, and very low frequency (VLF) transmitters were taken from *Subbotin et al.* [2011] and are scaled with *Kp*. The parameterization for the extremely low frequency (ELF) hiss waves, the grid size and other boundary conditions are the same as in *Drozdov et al.* [2015].

Figure 4 is similar to Figure 3 but for 3-D VERB simulations. Comparison between the simulations results (Figures 4d–4f and 4g–4i) and measurements (Figures 4a–4c) shows better agreement at different energies than in the case of 1-D simulations. In particular, the peak flux values at high energies (1.80 MeV) and the flux decay at low energies (0.59 MeV) are closer to the measurements of those in the case of 1-D simulations regardless of the radial diffusion rates. The difference between simulations with BA (Figures 4j–4l) and OZ (Figures 4m–4o) parameterizations is less pronounced than in the case of 1-D simulations (Figures 3j–4o). Figures 4j–4o show that the NDs (and LDs, that are shown in Figure S2) between model and observations are lower than in case of 1-D simulations, and the mean absolute value varies in the range of 26–34% in comparison to 33–51% in 1-D case. The mean absolute values of the difference between 3-D simulations with BA and OZ rates are 8% or less, while in the 1-D case, the mean absolute values of the same difference exceeded 11%.

The presented simulations show that the difference between 3-D simulations with different radial diffusion rates is smaller than the difference between each of the 3-D models and observations. The introduction of the local processes into the simulation provides better agreement with the observations, and the improvement does not strongly depend on the selection of radial diffusion coefficient model.

2.4. Sensitivity Tests

As discussed in section 1, a number of recent studies explored simulations with radial diffusion rates multiplied by a various constant up to 16. To investigate the applicability of this approach to a long-term simulation, we conduct a series of sensitivity tests using the VERB code. The sensitivity simulations discussed below have similar conditions as the simulations in sections 2.2 and 2.3. The sensitivity tests are performed for OZ radial diffusion rates D_{LL}^{O} multiplying or dividing by 2 and 3 in accordance with the variation described in by *Ozeke et al.* [2014].

Figure 5 shows observations of 1.04 MeV electron flux, results of 3-D simulations using original OZ radial diffusion rates, and OZ radial diffusion rates multiplied and divided by a factor of 3. The increased diffusion rates result in better agreement of the model (Figure 5d) and observations (Figure 5a) than the original OZ diffusion rates (Figure 5b) in the heart of the outer belt but produce an unrealistic "third" belt at $L = 2.5$ that is not seen in the observations (Figure 5a). In addition, the location of the third belt corresponds to the slot region which is usually devoid of relativistic electrons [*Fennell et al.*, 2015]. Better agreement of 3-D simulations and observations at higher L shells is likely a coincidence and generally cannot be considered as an improvement. Decreasing of diffusion rates leads to slower radial transport of electrons, which is consistent with our sensitivity test using a reduced radial diffusion rate (Figure 6c). The test shows that the electrons do not penetrate as low in L as observations show. The detailed results of sensitivity tests are shown in Figures S4–S7 for 1-D simulations and in Figures S8–S12 for 3-D simulations.

It is convenient to explore the effect of reduced and enhanced diffusion coefficients on simulations for a wide range of energies using the mean absolute value as a metric of comparison between simulation and observations. Figure 6 shows the dependence of the mean absolute value on energy for the sensitivity tests with original, reduced, and enhanced radial diffusion rates. Figure 6a presents the mean absolute values for the 1-D simulations, and Figure 6b is for 3-D simulations. The figure shows that multiplying or dividing radial diffusion parameterization D_{LL}^{O} by a constant number may improve 1-D simulations at a selected energy;

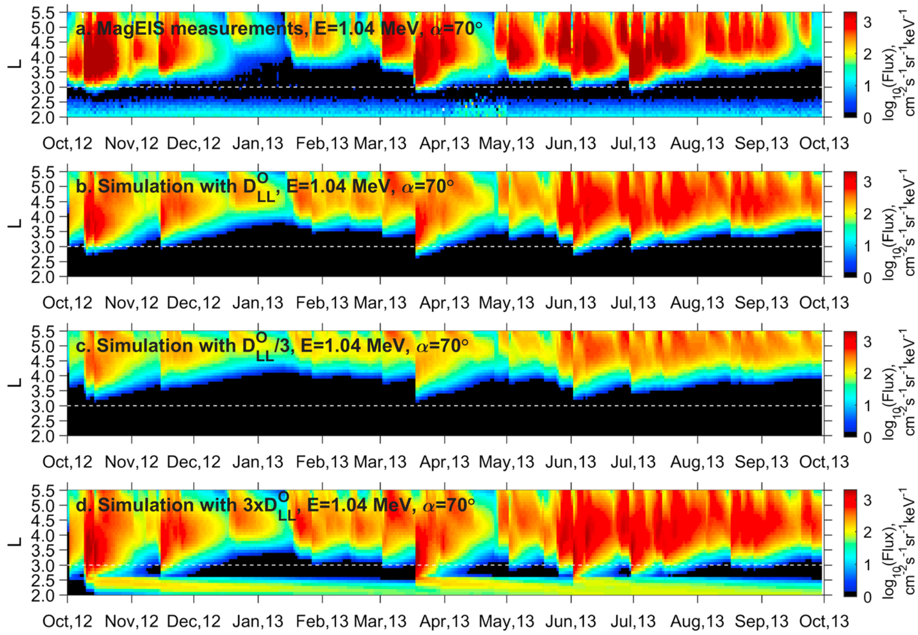

Figure 5. Electron flux profiles at 1.04 MeV and at pitch angle $\alpha = 70°$. (a) Van Allen Probe MagEIS measurements, (b) 3-D simulations with D_{LL}^{O}, (c) 3-D simulations with $D_{LL}^{O}/3$, and (d) 3-D simulations with $3\times D_{LL}^{O}$. The dashed line indicates L = 3.

however, results may be worse at other energies. The sensitivity tests for 3-D simulations do not improve the results of the modeling at all energies in comparison to the simulations with unmodified radial diffusion rates.

The approach of multiplying or dividing the radial diffusion rates by a constant number may help reproduce the dynamics in particular regions of space, and for particular energies, however, it is not likely to provide an

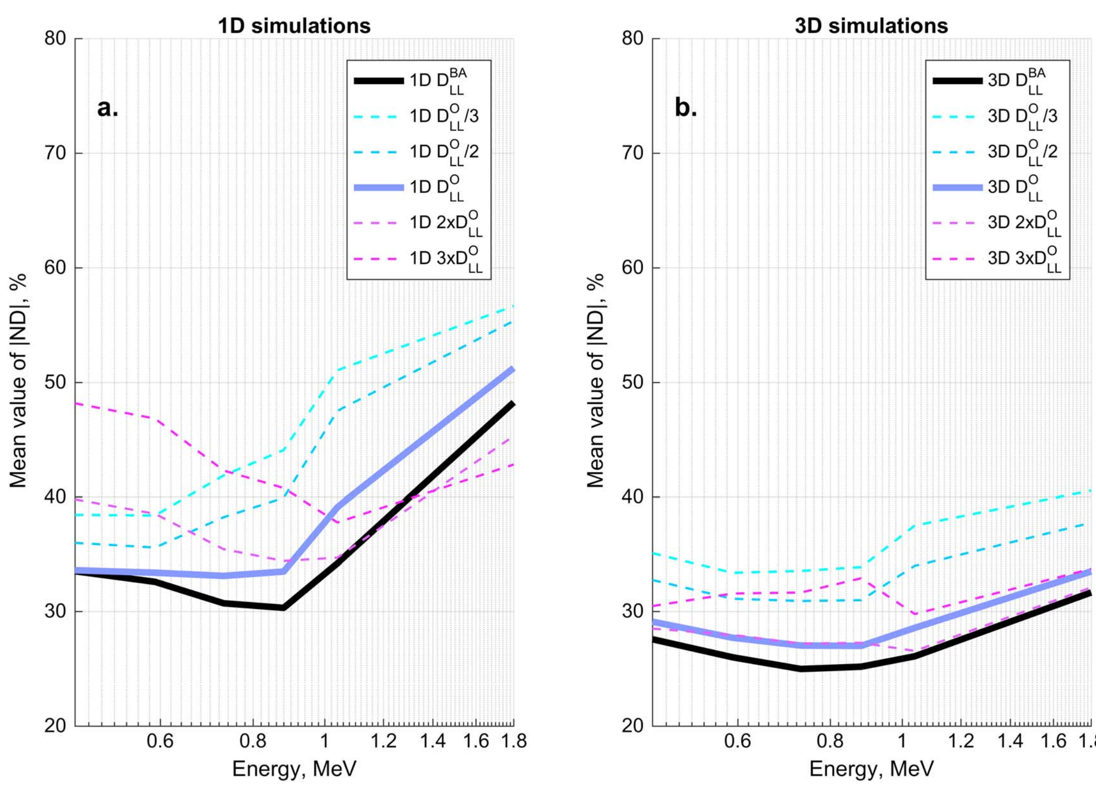

Figure 6. Variation of the mean absolute values versus energy for simulations with different radial diffusion rates. (a) 1-D simulations; (b) 3-D simulations.

overall improvement to the long-term 1-D and 3-D modeling results at different energies. Since the simulations with BA and with OZ parameterizations are practically indistinguishable, we can assume that this approach will not improve the results of the simulation with modified radial diffusion rate D_{LL}^{BA} from *Brautigam and Albert* [2000].

Several recent publications explored even more extreme modifications of the radial diffusion rates. In particular, a recent study by *Mann et al.* [2016] explored in their supporting information modification by a factor up to 16 and *Murphy et al.* [2016] suggested that "for any individual geomagnetic storm the actual diffusion rates could be 4 orders of magnitude smaller or larger than those predicted by an empirical model derived as a function of *Kp*," while the authors only suggested such variations for individual storms. We have to note, that the mean and median value of the storm time ULF wave power should not be interpreted as a fixed multiplication factor for the empirical radial diffusion rates. As Figures 5 and 6 clearly show, calculations with increased or decreased radial diffusion rates produce less accurate and unrealistic results. Although the radial diffusion rates can still be improved, both *Kp*-parametrized radial diffusion rates (BA and OZ) provided a good agreement of simulations with observations.

3. Discussion and Conclusions

In this study we have compared radial diffusion simulations with electromagnetic radial diffusion coefficients by *Brautigam and Albert* [2000] and with total radial diffusion coefficients of *Ozeke et al.* [2014]. One-dimensional simulations with realistic boundary conditions with either of the *Kp*-dependent radial diffusion coefficients capture the dynamics of the radiation belts. This result is consistent with previous studies [*Brautigam and Albert*, 2000; *Shprits et al.*, 2005; *Ozeke et al.*, 2014]. The difference between simulations is small in comparison with the measured variation of the electron fluxes. In the case of 3-D simulations that include local diffusion processes, the difference between simulations with different parameterizations of radial transport is further reduced. The outer electron radiation belt is a complex nonlinear system that shows a complicated and complex response to the change of each of the assumed parameters. In particular, full 3-D simulations appear to be less sensitive to the assumed radial diffusion rates than the simplified 1-D simulations. In addition, the description of realistic transport of the electrons can go beyond diffusion theory, especially for electrons at low energies, where convective transport is more important.

For space weather-related models, either parameterization can be used. The difference between the observations and models considered in the manuscript simulations are likely due to the inaccuracies associated with uncertainties of ELF/VLF wave models or missing physical processes such as magnetospheric convection.

The simulation results are in good agreement with the observations, which concludes that both models of radial diffusion are well suited for long-term 3-D modeling of the electron radiation belt dynamics. The incorporation of more accurate radial diffusion rates possibly validated by observations [e.g., *O'Brien et al.*, 2016] may improve the results of the simulation and should be a focus of further research. The parameters, and in particular radial diffusion rates, should not be fitted to reproduce observations in isolation from other processes. As shown by the sensitivity tests, a systematic increase or decrease even by a small number compared to scaling factors suggested in the literature deteriorated the simulation results at various energies.

Murphy et al. [2016] interprets the variability in the wave power as a variability in the radial diffusion rates. Further investigation of storm time ULF wave power is important, and the hourly power spectral density may at times reflect the rate of the radial diffusion. However, the radial diffusion is a slow process and assumes that at each particular moment, the changes in the third invariant are small. Consequently, the value of interest is an average wave power over a characteristic time scale associated with the radial transport and along the electrons drift trajectory. The radial diffusion transport is not likely fully defined by the ULF wave power observations at one or a few isolated areas. The violation of the third invariant causes the electron displacement in space and is the result of the interaction with ULF waves at various L shells and magnetic local times. Thus, effective wave power (for the actual diffusion rates) can be considerably less than the localized in space and time value of the wave power.

We have found in the current study that the two considered radial diffusion rates produce largely similar results, especially in 3-D simulations, as compared to observations at several energies. We demonstrated that great care must be taken in multiplying diffusion coefficients by a fixed factor to match observations at a particular energy, as although agreement may improve for the energy of interest, over several energies that agreement may be much worse. Lastly, we have illustrated that sensible limits should be enforced in any attempt to scale radial diffusion rates.

Acknowledgments
The authors used geomagnetic indices provided by OMNIWeb (http://omniweb.gsfc.nasa.gov/form/dx1.html) and are grateful to the RBSP-ECT team for the provision of Van Allen Probes observations (http://rbsp-ect.lanl.gov/). We would like to thank Dmitry Subbotin, Ksenia Orlova, and Hui Zhu for the useful discussion of the simulation details. We would like to acknowledge high-performance computing support from Yellowstone (ark:/85065/d7wd3xhc) provided by UCAR's Computational and Information System Laboratory, sponsored by the National Science Foundation and other agencies. This research was supported by NASA award NNX13E34G and NSF GEM AGS-1203747 and received funding support from the UC Office of the President, UC Lab Fees Research Program grant 12-LR-235337, and Horizon 2020 award 637302.

References

Albert, J. M., N. P. Meredith, and R. B. Horne (2009), Three-dimensional diffusion simulation of outer radiation belt electrons during the 9 October 1990 magnetic storm, *J. Geophys. Res.*, *114*, A09214, doi:10.1029/2009JA014336.

Blake, J. B., et al. (2013), The Magnetic Electron Ion Spectrometer (MagEIS) instruments aboard the Radiation Belt Storm Probes (RBSP) spacecraft, *Space Sci. Rev.*, *179*(1-4), 383–421, doi:10.1007/s11214-013-9991-8.

Brautigam, D. H., and J. M. Albert (2000), Radial diffusion analysis of outer radiation belt electrons during the October 9, 1990, magnetic storm, *J. Geophys. Res.*, *105*(A1), 291–309, doi:10.1029/1999JA900344.

Carpenter, D. L., and R. R. Anderson (1992), An ISEE/whistler model of equatorial electron density in the magnetosphere, *J. Geophys. Res.*, *97*(A2), 1097–1108, doi:10.1029/91JA01548.

Cornwall, J. M. (1968), Diffusion processes influenced by conjugate-point wave phenomena, *Radio Sci.*, *3*(7), 740–744, doi:10.1002/rds196837740.

Desorgher, L., P. Bühler, A. Zehnder, and E. O. Flückiger (2000), Simulation of the outer radiation belt electron flux decrease during the March 26, 1995, magnetic storm, *J. Geophys. Res.*, *105*(A9), 21,211–21,223, doi:10.1029/2000JA900060.

Drozdov, A. Y., Y. Y. Shprits, K. G. Orlova, A. C. Kellerman, D. A. Subbotin, D. N. Baker, H. E. Spence, and G. D. Reeves (2015), Energetic, relativistic, and ultrarelativistic electrons: Comparison of long-term VERB code simulations with Van Allen Probes measurements, *J. Geophys. Res. Space Physics*, *120*, 3574–3587, doi:10.1002/2014JA020637.

Fälthammar, C.-G. (1965), Effects of time-dependent electric fields on geomagnetically trapped radiation, *J. Geophys. Res.*, *70*(11), 2503–2516, doi:10.1029/JZ070i011p02503.

Fei, Y., A. A. Chan, S. R. Elkington, and M. J. Wiltberger (2006), Radial diffusion and MHD particle simulations of relativistic electron transport by ULF waves in the September 1998 storm, *J. Geophys. Res.*, *111*, A12209, doi:10.1029/2005JA011211.

Fennell, J. F., S. G. Claudepierre, J. B. Blake, T. P. O'Brien, J. H. Clemmons, D. N. Baker, H. E. Spence, and G. D. Reeves (2015), Van Allen Probes show that the inner radiation zone contains no MeV electrons: ECT/MagEIS data, *Geophys. Res. Lett.*, *42*, 1283–1289, doi:10.1002/2014GL062874.

Fok, M.-C., R. B. Horne, N. P. Meredith, and S. A. Glauert (2008), Radiation Belt Environment model: Application to space weather nowcasting, *J. Geophys. Res.*, *11*, A03S08, doi:10.1029/2007JA012558.

Kellogg, P. J. (1959), Van Allen radiation of solar origin, *Nature*, *183*, 1295–1297, doi:10.1038/1831295a0.

Kim, K.-C., D.-Y. Lee, Y. Shprits, H.-J. Kim, and E. Lee (2011), Electron flux changes in the outer radiation belt by radial diffusion during the storm recovery phase in comparison with the fully adiabatic evolution, *J. Geophys. Res.*, *116*, A09229, doi:10.1029/2011JA016642.

Lanzerotti, L. J., and C. G. Morgan (1973), ULF geomagnetic power near L = 4: 2. Temporal variation of the radial diffusion coefficient for relativistic electrons, *J. Geophys. Res.*, *78*, 4600–4610, doi:10.1029/JA078i022p04600.

Lanzerotti, L. J., and D. C. Webb (1978), Geomagnetic field fluctuations at synchronous orbit 2. Radial diffusion, *J. Geophys. Res.*, *83*(A8), 3866–3870, doi:10.1029/JA083iA08p03866.

Li, X. (2004), Variations of 0.7–6.0 MeV electrons at geosynchronous orbit as a function of solar wind, Space *Weather*, *2*, S03006, doi:10.1029/2003SW000017.

Lyons, L. R., and M. Schulz (1989), Access of energetic particles to storm time ring current through enhanced radial "diffusion,", *J. Geophys. Res.*, *94*(A5), 5491–5496, doi:10.1029/JA094iA05p05491.

Lyons, L. R., and R. M. Thorne (1973), Equilibrium structure of radiation belt electrons, *J. Geophys. Res.*, *78*(13), 2142–2149, doi:10.1029/JA078i013p02142.

Mann, I. R., et al. (2016), Explaining the dynamics of the ultra-relativistic third Van Allen radiation belt, *Nat. Phys.*, doi:10.1038/nphys3799.

Mauk, B. H., N. J. Fox, S. G. Kanekal, R. L. Kessel, D. G. Sibeck, and A. Ukhorskiy (2013), Science objectives and rationale for the Radiation Belt Storm Probes mission, *Space Sci. Rev.*, *179*(1–4), 3–27, doi:10.1007/s11214-012-9908-y.

Miyoshi, Y., A. Morioka, H. Misawa, T. Obara, T. Nagai, and Y. Kasahara (2003), Rebuilding process of the outer radiation belt during the 3 November 1993 magnetic storm: NOAA and Exos-D observations, *J. Geophys. Res.*, *108*(A1), 1004, doi:10.1029/2001JA007542.

Murphy, K. R., I. R. Mann, I. J. Rae, D. G. Sibeck, and C. E. J. Watt (2016), Accurately characterizing the importance of wave-particle interactions in radiation belt dynamics: The pitfalls of statistical wave representations, *J. Geophys. Res. Space Phys.*, 7895–7899, doi:10.1002/2016JA022618.

O'Brien, T. P., S. G. Claudepierre, T. B. Guild, J. F. Fennell, D. L. Turner, J. B. Blake, J. H. Clemmons, and J. L. Roeder (2016), Inner zone and slot electron radial diffusion revisited, *Geophys. Res. Lett.*, *43*, 7301–7310, doi:10.1002/2016GL069749.

Ozeke, L. G., I. R. Mann, and I. J. Rae (2009), Mapping guided Alfvén wave magnetic field amplitudes observed on the ground to equatorial electric field amplitudes in space, *J. Geophys. Res.*, *114*, A01214, doi:10.1029/2008JA013041.

Ozeke, L. G., I. R. Mann, K. R. Murphy, I. J. Rae, D. K. Milling, S. R. Elkington, A. A. Chan, and H. J. Singer (2012), ULF wave derived radiation belt radial diffusion coefficients, *J. Geophys. Res.*, *117*, A04222, doi:10.1029/2011JA017463.

Ozeke, L. G., I. R. Mann, K. R. Murphy, I. Jonathan Rae, and D. K. Milling (2014), Analytic expressions for ULF wave radiation belt radial diffusion coefficients, *J. Geophys. Res. Sapce Phys.*, *119*, 1587–1605, doi:10.1002/2013JA019204.

Rae, I. J., I. R. Mann, K. R. Murphy, L. G. Ozeke, D. K. Milling, A. A. Chan, S. R. Elkington, and F. Honary (2012), Ground-based magnetometer determination of in situ Pc4–5 ULF electric field wave spectra as a function of solar wind speed, *J. Geophys. Res.*, *117*, A04221, doi:10.1029/2011JA017335.

Reeves, G. D., D. N. Baker, R. D. Belian, J. B. Blake, T. E. Cayton, J. F. Fennell, R. H. W. Friedel, M. M. Meier, R. S. Selesnick, and H. E. Spence (1998), The global response of relativistic radiation belt electrons to the January 1997 magnetic cloud, *Geophys. Res. Lett.*, *25*(17), 3265–3268, doi:10.1029/98GL02509.

Reeves, G. D., K. L. McAdams, R. H. W. Friedel, and T. P. O'Brien (2003), Acceleration and loss of relativistic electrons during geomagnetic storms, *Geophys. Res. Lett.*, *30*(10), 1529, doi:10.1029/2002GL016513.

Reeves, G. D., Y. Chen, G. S. Cunningham, R. W. H. Friedel, M. G. Henderson, V. K. Jordanova, J. Koller, S. K. Morley, M. F. Thomsen, and S. Zaharia (2012), Dynamic Radiation Environment Assimilation Model: DREAM, *Space Weather*, *10*, S03006, doi:10.1029/2011SW000729.

Roederer, J. G. (1970), *Dynamics of Geomagnetically Trapped Radiation*, Springer, Berlin Heidelberg.

Schulz, M., and L. J. Lanzerotti (1974), *Particle Diffusion in the Radiation Belts*, Phys. and Chem. in Space, Springer, New York.

Shprits, Y. Y., and R. M. Thorne (2004), Time dependent radial diffusion modeling of relativistic electrons with realistic loss rates, *Geophys. Res. Lett.*, *31*, L08805, doi:10.1029/2004GL019591.

Shprits, Y. Y., R. M. Thorne, G. D. Reeves, and R. Friedel (2005), Radial diffusion modeling with empirical lifetimes: comparison with CRRES observations, *Ann. Geophys.*, *23*(4), 1467–1471, doi:10.5194/angeo-23-1467-2005.

Shprits, Y. Y., R. M. Thorne, R. Friedel, G. D. Reeves, J. Fennell, D. N. Baker, and S. G. Kanekal (2006), Outward radial diffusion driven by losses at magnetopause, *J. Geophys. Res.*, *111*, A11214, doi:10.1029/2006JA011657.

Shprits, Y. Y., D. A. Subbotin, N. P. Meredith, and S. R. Elkington (2008a), Review of modeling of losses and sources of relativistic electrons in the outer radiation belt II: Local acceleration and loss, *J. Atmos. Sol. Terr. Phys.*, *70*(14), 1694–1713, doi:10.1016/j.jastp.2008.06.014.

Shprits, Y. Y., S. R. Elkington, N. P. Meredith, and D. A. Subbotin (2008b), Review of modeling of losses and sources of relativistic electrons in the outer radiation belt I: Radial transport, *J. Atmos. Sol. Terr. Phys.*, *70*(14), 1679–1693, doi:10.1016/j.jastp.2008.06.008.

Stratton, J. M., R. J. Harvey, and G. A. Heyler (2014), Mission overview for the Radiation Belt Storm Probes mission, in *The Van Allen Probes Mission*, edited by N. Fox and J. L. Burch, pp. 29–57, Springer US, Boston, Mass.

Su, Z., F. Xiao, H. Zheng, and S. Wang (2010), STEERB: A three-dimensional code for storm-time evolution of electron radiation belt, *J. Geophys. Res.*, *115*, A09208, doi:10.1029/2009JA015210.

Su, Z., et al. (2015), Ultra-low-frequency wave-driven diffusion of radiation belt relativistic electrons, *Nat. Commun.*, *6*, 10096, doi:10.1038/ncomms10096.

Subbotin, D., Y. Shprits, and B. Ni (2010), Three-dimensional VERB radiation belt simulations including mixed diffusion, *J. Geophys. Res.*, *115*, A03205, doi:10.1029/2009JA015070.

Subbotin, D. A., and Y. Y. Shprits (2009), Three-dimensional modeling of the radiation belts using the Versatile Electron Radiation Belt (VERB) code, *Space Weather*, *7*, S10001, doi:10.1029/2008SW000452.

Subbotin, D. A., and Y. Y. Shprits (2012), Three-dimensional radiation belt simulations in terms of adiabatic invariants using a single numerical grid, *J. Geophys. Res.*, *117*, A05205, doi:10.1029/2011JA017467.

Subbotin, D. A., Y. Y. Shprits, and B. Ni (2011), Long-term radiation belt simulation with the VERB 3-D code: Comparison with CRRES observations, *J. Geophys. Res.*, *116*, A12210, doi:10.1029/2011JA017019.

Tu, W., X. Li, Y. Chen, G. D. Reeves, and M. Temerin (2009), Storm-dependent radiation belt electron dynamics, *J. Geophys. Res.*, *114*, A02217, doi:10.1029/2008JA013480.

Tu, W., G. S. Cunningham, Y. Chen, M. G. Henderson, E. Camporeale, and G. D. Reeves (2013), Modeling radiation belt electron dynamics during GEM challenge intervals with the DREAM3D diffusion model, *J. Geophys. Res. Atmos.*, *118*, 6197–6211, doi:10.1002/jgra.50560.

Turner, D. L., Y. Shprits, M. Hartinger, and V. Angelopoulos (2012), Explaining sudden losses of outer radiation belt electrons during geomagnetic storms, *Nat. Phys.*, *8*(3), 208–212, doi:10.1038/nphys2185.

Vampola, A. L., J. V. Osborn, and B. M. Johnson (1992), CRRES magnetic electron spectrometer AFGL-701-5A (MEA), *J. Spacecr. Rockets*, *29*(4), 592–595, doi:10.2514/3.25504.

Van Allen, J. A., and L. A. Frank (1959), Radiation around the Earth to a radial distance of 107,400 km, *Nature*, *183*(4659), 430–434, doi:10.1038/183430a0.

Varotsou, A., D. Boscher, S. Bourdarie, R. B. Horne, N. P. Meredith, S. A. Glauert, and R. H. Friedel (2008), Three-dimensional test simulations of the outer radiation belt electron dynamics including electron-chorus resonant interactions, *J. Geophys. Res.*, *113*, A12212, doi:10.1029/2007JA012862.

Walt, M. (1970), Radial diffusion of trapped particles, in *Particles and Fields in the Magnetosphere*, pp. 410–415, Springer, Netherlands.